The 8th European Congress on Computational Methods in Applied Sciences and Engineering
ECCOMAS Congress 2022
5-–9 June 2022, Oslo, Norway

A COUPLED MULTIPHYSICS APPROACH FOR MODELING IN-STENT RESTENOSIS

Kiran Manjunatha[1], Marek Behr[2], Felix Vogt[1] and Stefanie Reese[1*]

[1] Institute of Applied Mechanics (IFAM)
RWTH Aachen University
Mies-van-der-Rohe-Str. 1, 52074 Aachen, Germany
[*] corresponding author, email: stefanie.reese@ifam.rwth-aachen.de

[2] Chair for Computational Analysis of Tehcnical Systems (CATS)
RWTH Aachen University
Schinkelstraße 2, 52062 Aachen, Germany

[3] Department of Cardiology, Pulmonology, Intensive Care and Vascular Medicine
RWTH Aachen University
Pauwelsstraße 30, Aachen, Germany

Key words: in-stent restenosis, growth factors, smooth muscle cells, extracellular matrix, drug-eluting stents, rapamycin, pharmacokinetics, pharmacodynamics

Abstract. Drug-eluting stents were developed to counteract the severe restenosis observed after bare-metal stent implantation. The risk of restenosis still prevailed due to the inhibitory effect of the drug on endothelial healing. The current work focuses on extending a multiphysics-based modeling framework to include the effect of anti-inflammatory drugs embedded in the drug-eluting stents. An additional advection-reaction-diffusion equation governing the drug transport is introduced herein. Additionally, the effect of drugs, specifically rapamycin-based ones, on the proliferation of smooth muscle cells is captured. An optimal level of drug embedment is realized through the modeling framework.

1 INTRODUCTION

Percutaneous coronary intervention (PCI) is a minimally invasive procedure wherein the plaque built up within the coronary arteries, as part of an inflammatory pathosis termed *atherosclerosis*, is compressed against the coronary arterial walls using balloon angioplasty, and subsequently, a supporting scaffold called a stent is placed to restore normal blood flow within the coronary artery. Endothelial denudation and overstretch injuries caused during the PCI procedure kick start various signaling cascades within the arterial wall resulting in uncontrolled tissue growth and formation of obstructions to the blood flow. The condition is termed in-stent restenosis and the mechanism associated is called neointimal hyperplasia. A multiphysics modeling framework to replicate restenosis by tracking the pathophysiology's significant players, including the platelet-derived growth factor (PDGF), the transforming growth factor (TGF)$-\beta$, the extracellular matrix (ECM) and the smooth muscle cells (SMCs), was presented

in [5]. Due to the advent of drug-eluting stents (DES), the restenosis rates were considerably reduced compared to those after a bare-metal stent (BMS) implantation. DESs contain a polymer layer around the metallic core of their struts wherein an anti-inflammatory drug is embedded. Although DESs were expected to eradicate the occurence of restenosis, the probability of its occurence still remains statistically significant. This is suspected mainly due to the growth-inhibitory mechanisms acting indiscriminately on the SMCs as well as the endothelial cells, delaying the healing of the endothelium. The current work is thus aimed at extending the modeling framework presented in [5] to include pharmacokinetics and pharmacodynamics in the arterial wall due to a DES implantation. The extended fidelity could then serve as an *in silico* model for interventional cardiologists to tune DES implantation parameters.

2 METHODOLOGY

The pathophysiological hypothesis behind the model for in-stent restenosis observed after implantation of a bare metal stent (BMS) is presented in [5]. The modeling framework presented therein is extended here to capture the pharmacokinetics and pharmacodynamics involved in the pathology of restenosis after implantation of a DES. A schematic of the extended modeling framework is presented in Fig. 1.

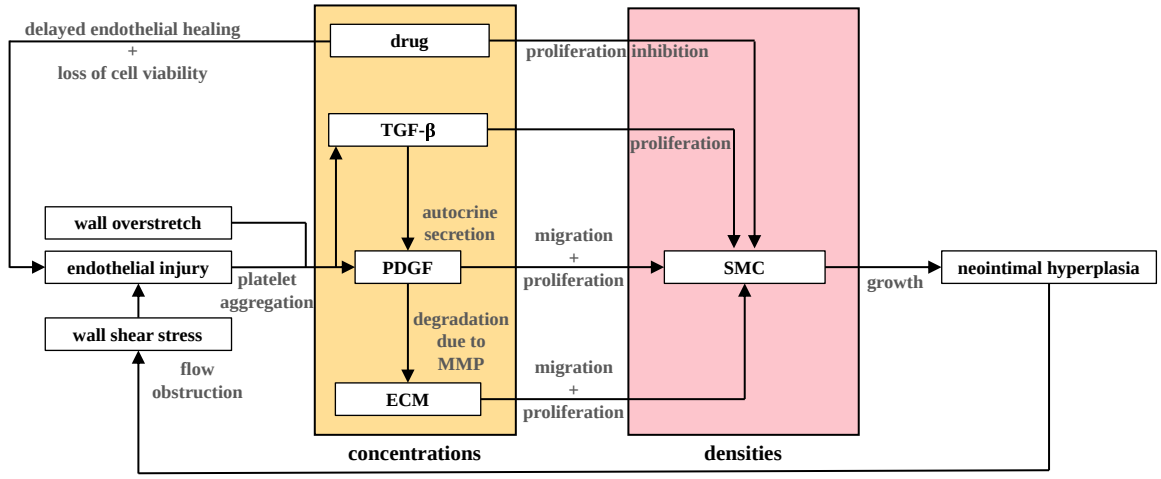

Figure 1: **Schematic of the restenotic process**

2.1 Evolution of wall species

The cellular species (SMCs) of the arterial wall are quantified in terms of cell densities (ρ_S), while the extracellular species (PDGF, TGF$-\beta$, ECM, and the drug) are quantified in terms of their concentrations (c_P,c_T,c_E, and c_D). The arterial wall is modeled as an open system. The Eulerian forms of the advection-reaction-diffusion equations that govern the evolution of the species within the vessel wall are established based on the biochemical interactions involved in the pathophysiology of restenosis. Those that govern the evolution of c_P,c_T, and c_E remain the

same as in [5], and are summarised here without elaboration (Eqs. 1, 2, and 3).

$$\left.\frac{\partial c_{_P}}{\partial t}\right|_{\boldsymbol{x}} + \mathsf{div}\,(c_{_P}\,\boldsymbol{v}) \;=\; \underbrace{\mathsf{div}\,(D_{_P}\,\mathsf{grad}\,c_{_P})}_{\text{diffusion}} + \underbrace{\eta_{_P}\,\rho_{_S}\,c_{_T}}_{\substack{\text{autocrine secretion}\\ \text{by SMCs}}} - \underbrace{\varepsilon_{_P}\,f_{_T}\,\rho_{_S}\,c_{_P}}_{\substack{\text{receptor}\\ \text{internalization}}}, \tag{1}$$

$$\left.\frac{\partial c_{_T}}{\partial t}\right|_{\boldsymbol{x}} + \mathsf{div}\,(c_{_T}\,\boldsymbol{v}) \;=\; \underbrace{\mathsf{div}\,(D_{_T}\,\mathsf{grad}\,c_{_T})}_{\text{diffusion}} - \underbrace{\varepsilon_{_T}\,\rho_{_S}\,c_{_T}}_{\substack{\text{receptor}\\ \text{internalization}}}\;, \tag{2}$$

$$\left.\frac{\partial c_{_E}}{\partial t}\right|_{\boldsymbol{x}} + \mathsf{div}\,(c_{_E}\,\boldsymbol{v}) \;=\; \underbrace{\eta_{_E}\rho_{_S}\left(1-\frac{c_{_E}}{c_{_{E,th}}}\right)}_{\substack{\text{secretion by}\\ \text{synthetic SMCs}}} - \underbrace{\varepsilon_{_E}\,c_{_P}\,c_{_E}}_{\substack{\text{MMP-induced}\\ \text{degradation}}}\;, \tag{3}$$

The additional species that influences the inflammatory response of the vessel wall after DES implantation, and hence being plugged into the earlier developed modeling framework, is the drug embedded within the stent. Within this work, a rapamycin-based drug (sirolimus/everolimus) is considered to be embedded within a polymer layer coated on the metallic core of the DES. This drug is considered diffusive in the vessel wall. An additional sink term takes care of the internalization of targeted receptors for the drug on the SMCs, which results in deterioration of drug presence. Hence, the evolution equation for the drug reads as shown in Eq. 4 below, which reads

$$\left.\frac{\partial c_{_D}}{\partial t}\right|_{\boldsymbol{x}} + \mathsf{div}\,(c_{_D}\,\boldsymbol{v}) \;=\; \underbrace{\mathsf{div}\,(D_{_D}\,\mathsf{grad}\,c_{_D})}_{\text{diffusion}} - \underbrace{\varepsilon_{_D}\,\rho_{_S}\,c_{_D}}_{\substack{\text{receptor}\\ \text{internalization}}}\;, \tag{4}$$

where $\varepsilon_{_D}$ is termed the receptor internalization coefficient for the drug. Rapamycin is known to arrest cell-cycle progression, mainly of SMCs, at the G1 phase. This results in an antiproliferative effect on SMCs, which shall be modeled by multiplying an additional drug-dependant scaling function $f_{_D}$ to the proliferation term for SMCs within the evolution equation (Eq. 5), which reads

$$\begin{aligned}\left.\frac{\partial \rho_{_S}}{\partial t}\right|_{\boldsymbol{x}} + \mathsf{div}\,(\rho_{_S}\,\boldsymbol{v}) \;=\; & \underbrace{-\,\mathsf{div}\left(\chi_{_C}\left(1-\frac{c_{_E}}{c_{_{E,th}}}\right)\rho_{_S}\,\mathsf{grad}\,c_{_P}\right)}_{\text{chemotaxis}} \\ & + \underbrace{\mathsf{div}\,(\chi_{_H}\,f_{_P}\,\rho_{_S}\,\mathsf{grad}\,c_{_E})}_{\text{haptotaxis}} + \underbrace{\eta_{_S}\,f_{_T}\,f_{_D}\,c_{_P}\,\rho_{_S}\left(1-\frac{c_{_E}}{c_{_{E,th}}}\right)}_{\text{proliferation}}.\end{aligned} \tag{5}$$

The effect of rapamycin on migratory mechanisms of SMCs is ignored in the current work. The scaling function $f_{_D}$ can be prescribed based on experimental determination of the function that

quantitatively describes the dose-dependent inhibitory effect of the drug accurately. An example would be of the following form determined in [7],

$$f_{_D} = \frac{\beta\,(c_{_D})^{\alpha} + A^{\alpha}}{(c_{_D})^{\alpha} + A^{\alpha}}, \tag{6}$$

where the parameters α, β, and A are fit to experimental results. Additionally, Eqs. 1 and 5 utilize the sigmoidal scaling functions $f_{_P}$ and $f_{_T}$ to switch biochemical phenomena between their on and off states, which are defined as

$$f_{_P} := \frac{1}{1 + e^{-l_{_P}\left(c_{_P} - c_{_{P,th}}\right)}}, \tag{7}$$

$$f_{_T} := \frac{1}{1 + e^{l_{_T}\left(c_{_T} - c_{_{T,th}}\right)}}. \tag{8}$$

2.2 Continuum mechanical modeling

The structural behavior of the arterial wall is assumed to be predominantly influenced by the medial and adventitial layers, and each layer is assumed to be composed of two families of collagen fibres embedded in an isotropic ground matrix. SMCs are considered to be the drivers of the growth process within the isotropic ground matrix, while collagen is assumed to modulate the compliance of the arterial wall. Balance of linear momentum is considered to govern the mechanical equilibrium, considering that the growth process is slow and hence quasi-static.

2.2.1 Kinematics

A particle at position $\boldsymbol{X}$ in the reference configuration is mapped to that at $\boldsymbol{x}$ in the current configuration via the deformation gradient $\boldsymbol{F} = \partial\,\boldsymbol{\varphi}(\boldsymbol{X}, t)/\partial\boldsymbol{X}$, where $\boldsymbol{\varphi}$ is the deformation map between the configurations. The right Cauchy-Green tensor is further defined as $\boldsymbol{C} = \boldsymbol{F}^{T}\,\boldsymbol{F}$. For the description of growth, the well established multiplicative decomposition of the deformation gradient is adopted, i.e.

$$\boldsymbol{F} = \boldsymbol{F}_e\,\boldsymbol{F}_g = \underbrace{\boldsymbol{F}_e\,\boldsymbol{R}_g}_{:=\boldsymbol{F}_*}\,\boldsymbol{U}_g = \boldsymbol{F}_*\,\boldsymbol{U}_g, \tag{9}$$

wherein an intermediate incompatible configuration which achieves a locally stress-free state is assumed, and the elastic deformation gradient $\boldsymbol{F}_e$ ensures the compatibility of the total deformation in the continuum. $\boldsymbol{R}_g$ is an orthogonal tensor representing the rotational part of $\boldsymbol{F}_g$, and $\boldsymbol{U}_g$ is the right stretch tensor associated with growth [3]. Also,

$$\boldsymbol{C}_* = \boldsymbol{F}_*^{T}\,\boldsymbol{F}_* = \boldsymbol{U}_g^{-1}\,\boldsymbol{C}\,\boldsymbol{U}_g^{-1}. \tag{10}$$

The volumetric change associated with the deformation gradient $\boldsymbol{F}$ can also be split into its growth and elastic parts as

$$J = \mathsf{det}\,\boldsymbol{F} = \mathsf{det}\,\boldsymbol{F}_e\;\mathsf{det}\,\boldsymbol{F}_g = \mathsf{det}\,\boldsymbol{F}_*\;\mathsf{det}\,\boldsymbol{U}_g = J_e\,J_g. \tag{11}$$

2.2.2 Helmholtz free energy

The Helmholtz free energy per unit volume in the reference configuration is split into an isotropic part associated with the isotropic ground matrix, and an anisotropic part corresponding to the collagen fibers, i.e.,

$$\psi = \psi_{iso}(\boldsymbol{C}, \boldsymbol{U}_g) + \psi_{ani}(\boldsymbol{C}, \boldsymbol{H}_1, \boldsymbol{H}_2, c_{_E}^0). \tag{12}$$

The specific choices for the aforementioned parts of the Helmholtz free energy are given by the Neo-Hookean form

$$\psi_{iso}(\boldsymbol{C}, \boldsymbol{U}_g) = \frac{\mu}{2}\left(\operatorname{tr}\boldsymbol{C}_* - 3\right) - \mu \ln J_e + \frac{\Lambda}{4}\left(J_e^2 - 1 - 2\ln J_e\right), \tag{13}$$

and the exponential form [4]

$$\psi_{ani}(\boldsymbol{C}, \boldsymbol{H}_1, \boldsymbol{H}_2, c_{_E}^0) = \frac{k_1}{2k_2}\sum_{i=1,2}\left(\mathsf{exp}\left[k_2\langle E_i\rangle^2\right] - 1\right). \tag{14}$$

The stress-like material parameter k_1 above is here designed to be a linear function of the local ECM concentration in the reference configuration $c_{_E}^0$, i.e.,

$$k_1 = \bar{k}_1\left(\frac{c_{_E}^0}{c_{_{E,eq}}}\right), \tag{15}$$

where $\bar{k}_1$ is the stress-like material parameter for healthy collagen and $c_{_{E,eq}}$ is the homeostatic ECM concentration in a healthy artery. $\boldsymbol{H}_i$ $(i = 1, 2)$ are the generalized structural tensors constructed from local collagen orientations $\boldsymbol{a}_{0i}$ in the reference configuration using

$$\boldsymbol{H}_i \;=\; \kappa\,\boldsymbol{I} + (1 - 3\,\kappa)\;\boldsymbol{a}_{0i}\otimes\boldsymbol{a}_{0i}\;, \tag{16}$$

where κ is a dispersion parameter [2]. The Green-Lagrange strain E_i is defined as

$$E_i := \boldsymbol{H}_i : \boldsymbol{C} - 1. \tag{17}$$

The first Piola-Kirchhoff stress tensor is deduced from the Helmholtz free energy function using

$$\boldsymbol{P} = \frac{\partial\psi}{\partial\boldsymbol{F}}. \tag{18}$$

2.2.3 Growth modeling

The right stretch tensor $\boldsymbol{U}_g$, appearing in Eq. 13, can be prescribed as a function of the local SMC density in the reference configuration $\rho_{_S}^0$, i.e.,

$$\boldsymbol{U}_g := \boldsymbol{U}_g(\rho_{_S}^0). \tag{19}$$

Specific forms of $\boldsymbol{U}_g$ are suggested in [5] based on histological inferences.

variable	initial condition ($\forall \boldsymbol{x} \in \Omega$)
$c_{_P}$	0
$c_{_T}$	0
$c_{_E}$	$c_{_{E,eq}}$
$c_{_D}$	0
$\rho_{_S}$	$\rho_{_{S,eq}}$

Table 1: **Initial conditions**

2.3 Initial and boundary conditions

The initial ECM concentrations and SMC densities are prescribed to be those of a healthy homeostatic vessel in equilibrium. PDGF, TGF$-\beta$, and the drug are considered initially absent in the vessel wall. Table 1 summarizes the relevant initial conditions.

All the relevant boundary conditions are summarized in Table 2.

(a) PDGF and TGF-β enter the arterial wall as a consequence of platelet aggregation after endothelial denudation via stent implantation. This effect can be modeled by prescribing influxes along the normal $\boldsymbol{n}$ at the injury sites on the vessel wall which are not in contact with the DES, and hence exposed directly to the blood flow ($\Gamma^N_{_{GF}}$). These influxes are directly prescribed as time-varying profiles, dependent on the load-factor ${}^1l_{_f}$ and the peak influx $\bar{q}^{\text{ref}}_{_{GF}}$. $GF = P, T$, appearing in the subscripts of the aforementioned boundary variable and the peak influx variable, refer to those corresponding to PDGF and TGF$-\beta$ respectively. Homogeneous Neumann boundary conditions are applied on the boundaries of the vessel wall are in contact with the DES ($\Gamma^N_{_D}$) as well as the remaining boundaries ($\Gamma^N_{_R}$) on the vessel wall. Total boundary in the current configuration is hence $\Gamma = \Gamma^N_{_{GF}} \cup \Gamma^N_{_D} \cup \Gamma^N_{_R}$.

(b) The drug is assumed to enter the vessel wall at regions where the DES is in contact with the vessel wall ($\Gamma^N_{_D}$). Drug influx is again prescribed as a time-varying profile, dependent on the load-factor ${}^2l_{_f}$ and the peak influx $\bar{q}^{\text{ref}}_{_D}$.

(c) The ECM and the SMCs are considered to be restrained within the arterial wall and hence homogenous Neumann boundary conditions are prescribed on the entire boundary of the system Γ.

(c) Displacements are prescribed on the boundary $\Gamma_{0,u}$ in the reference configuration, and tractions on the boundary $\Gamma_{0,T}$ in the reference configuration. Also, the total boundary in the reference configuration $\Gamma_0 = \Gamma_{0,u} \cup \Gamma_{0,T}$.

Additional drug can enter the vessel wall due to downstream deposition from blood flow and lipophilicity of the drug. This effect is currently not modeled.

	variable	Dirichlet	Neumann
(a)	c_P	–	$\boldsymbol{q}_P \cdot \boldsymbol{n} = -D_P \,\mathsf{grad}\,(c_P) \cdot \boldsymbol{n} = \bar{q}_P = {}^1l_f(t)\,\bar{q}_P^{\mathrm{ref}}$ on Γ_{GF}^N
			$\mathsf{grad}\,(c_P) \cdot \boldsymbol{n} = 0$ on $\Gamma_D^N \cup \Gamma_R^N$
	c_T	–	$\boldsymbol{q}_T \cdot \boldsymbol{n} = -D_T \,\mathsf{grad}\,(c_T) \cdot \boldsymbol{n} = \bar{q}_T = {}^1l_f(t)\,\bar{q}_T^{\mathrm{ref}}$ on Γ_{GF}^N
			$\mathsf{grad}\,(c_T) \cdot \boldsymbol{n} = 0$ on $\Gamma_D^N \cup \Gamma_R^N$
(b)	c_D	–	$\boldsymbol{q}_D \cdot \boldsymbol{n} = -D_D \,\mathsf{grad}\,(c_D) \cdot \boldsymbol{n} = \bar{q}_D = {}^2l_f(t)\,\bar{q}_D^{\mathrm{ref}}$ on Γ_D^N
			$\mathsf{grad}\,(c_D) \cdot \boldsymbol{n} = 0$ on $\Gamma_{GF}^N \cup \Gamma_R^N$
(c)	c_E	–	$\mathsf{grad}\,(c_E) \cdot \boldsymbol{n} = 0$ on Γ
	ρ_S	–	$\mathsf{grad}\,(\rho_S) \cdot \boldsymbol{n} = 0$ on Γ
(d)	$\boldsymbol{u}$	$\boldsymbol{u} = \hat{\boldsymbol{u}}$ on $\Gamma_{0,u}$	$\boldsymbol{T} = \boldsymbol{P} \cdot \boldsymbol{N} = \hat{\boldsymbol{T}}$ on $\Gamma_{0,T}$

Table 2: **Boundary conditions**

Presence of rapamycin-based drugs on the endothelium results in reduction of endothelial cell-viability as well as increased permeability of the wall to blood contents [1] (Fig. 1). Also, low local wall-shear-stresses can result in higher stagnation period of the blood, and hence higher influx of growth factors into the vessel wall. To capture these effects, the time-dependent load-factor profile ${}^1l_f$ is chosen to be of the form

$$l_f(t) := H \exp\left(-\frac{t}{t_1}\right)\left(1 - \exp\left(-\frac{t}{t_2}\right)\right), \tag{20}$$

where H refers to the amplitude, t_1 and t_2 are time-like parameters which control the curvature of the influx profile. t_1 is calculated as

$$t_1 := t_2 \exp\left(\frac{t_p}{t_2}\right) - t_2, \tag{21}$$

where t_p can be considered the time required to achieve peak influx of the given quantity, which is in turn dependent on the local wall-shear-stress ($\boldsymbol{\tau}_W$) and the drug concentration (c_D) on the endothelium, i.e.,

$$t_p := t_p(\boldsymbol{\tau}_W, c_D). \tag{22}$$

The load-factor profile for the drug influx from the DES into the vessel wall ${}^2l_f(t)$ is also modeled using Eq. 20. The parameters t_p and t_2 are chosen in such a way that the cumulative drug-release profiles available for the specific drug are matched with that shown in Fig. 2b.

The time-dependent load-factor profiles for varying levels of $\boldsymbol{\tau}_W$ and c_D are shown in Fig. 2a. Additionally, the cumulative integral of the load-factor function is shown in Fig. 2b.

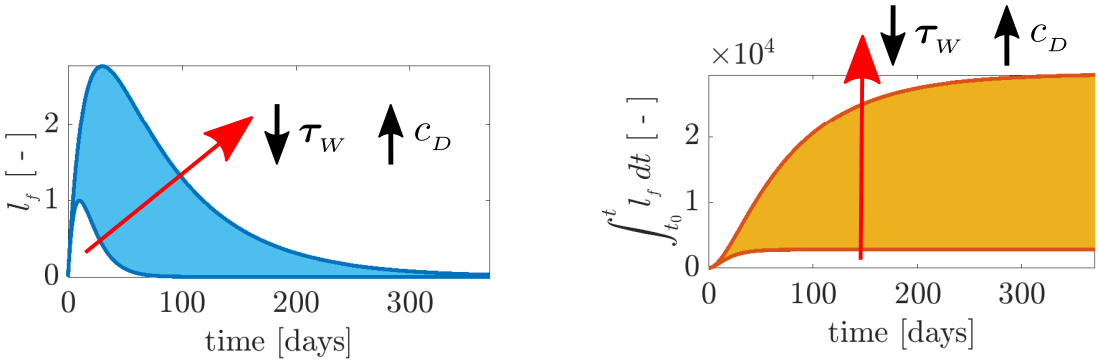

(a) load-factor profiles

(b) cumulative integral of the load-factor

Figure 2: **Time-varying load-factor profiles and their cumulative integrals depending on wall-shear-stress (τ_W) and drug concentration (c_D) on the endothelium**

2.4 Finite element implementation

Eqs. 1-5 are first transformed to their Lagrangian equivalents to couple them with the Lagrangian form of the balance of linear momentum. The boundary conditions listed in Table 2 are also transferred to the Lagrangian setting. Spatial discretization is performed using trilinear hexahedral elements and the temporal discretization is performed via the implicit backward Euler method. The resulting non symmetric monolithic system is iteratively solved via the Newton-Raphson method.

3 NUMERICAL EVALUATION

A quadrant of an artery is modeled with the boundary conditions depicted in Fig. 3. Medial layer is represented in red, while the adventitial layer is represented in green. Endothelium on a region (in blue) on the luminal surface is considered denuded due to DES implantation, and hence PDGF and TGF$-\beta$ influxes are prescribed on this region. An idealized stent-strut geometry is assumed. The contact area between the stent strut and the vessel wall (region in orange) is restrained against displacements in all directions. Drug influx is also prescribed on this region. Initial ECM concentration and SMC density are set to those of a healthy artery.

Fig. 4 depicts the distribution of the growth stretch variable ϑ, which is calculated using $\boldsymbol{U}_g$, under the absence of drug-elution. The variation in the thickness of neointima formed due to the restenotic process for varying levels of drug embedded in the polymer layer of the DES is plotted in Fig. 5. It is realized from this figure that at $q_D^{\text{ref}} = 50$ [nmol/mm^2/day], the restenotic growth is minimum.

4 CONCLUSION

The current work is aimed at extending the in-stent restenosis modeling framework presented in [5] to include pharmacokinetics and pharmacodynamics of a rapamycin-based drug embedded within the polymer layer of a DES. The drug has contradictory effects on the process of

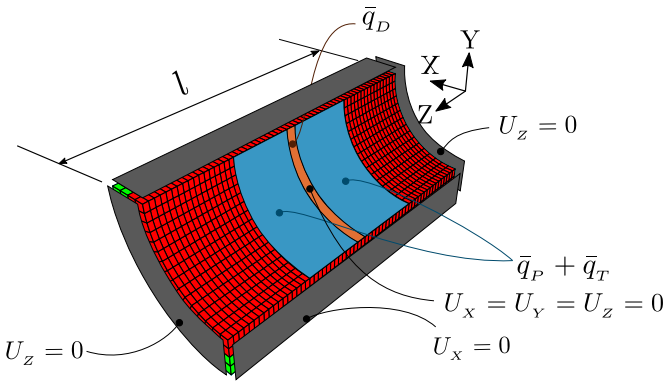

Figure 3: **Boundary conditions**

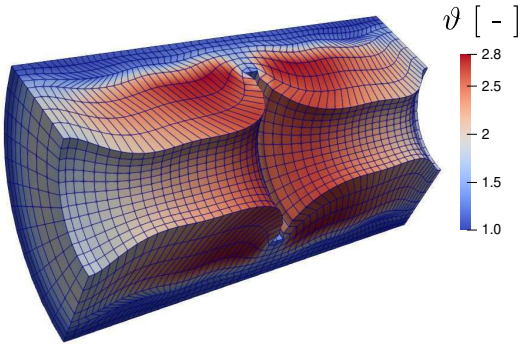

Figure 4: **Growth stretch (ϑ) distribution without drug-elution**

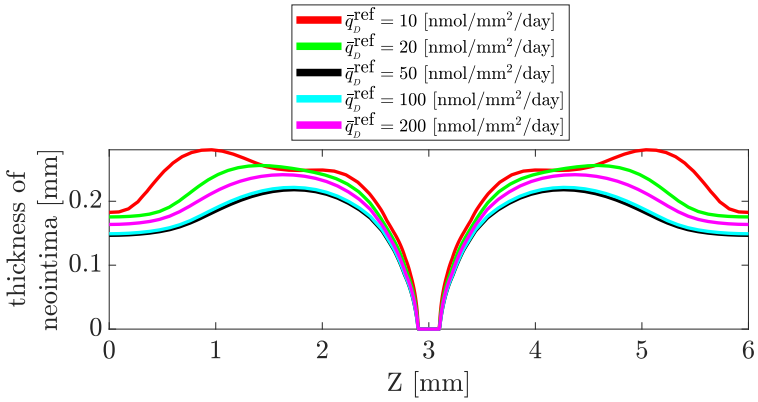

Figure 5: **Thickness of the neointima formed along the longitudinal direction for varying levels of drug-elution**

restenosis. This is atttributed to the inhibitory effect that it imparts on not only the SMCs but also the endothelial cells, which results in delayed endothelial regeneration. These counteracting effects point towards an optimal amount of drug-embedment in the DES that will lead to minimal restenosis. Therefore, this extended framework is aimed to serve as an *in silico* model for assessing patient specific risks associated with restenosis, and subsequently provide the interventional cardiologists with an optimal set of DES implantation parameters, including the amount of drug embedded on the DES. Patient-specific aspects can be embedded into the model via the wide array of parameters which can be physiologically determined.

5 ACKNOWLEDGEMENTS

Financial support provided by the German Research Foundation (DFG) for the subproject "In-stent restenosis in coronary arteries - in silico investigations based on patient-specific data and meta modeling" (project number 465213526) of SPP2311 is gratefully acknowledged. In addition, we acknowledge the financial support from DFG through projects 395712048 and 403471716.

REFERENCES

[1] Barilli, A., Visigalli, R., Sala, R., Gazzola, G. C., parolari, A., Tremoli, E., Bonomini, S., Simon, A., Closs, I. C., Dall´Asta, V. and Bussolati, O. In human endothelial cells rapamycin causes mTORC2 inhibition and impairs cell viability and function. *Cardiovascular Research* (2008) **78**:563–571.

[2] Gasser, T. C., Ogden, R. W. and Holzapfel, G. A. Hyperelastic modelling of arterial layers with distributed collagen fibre orientations. *Journal of the Royal Society Interface* (2006) **3(6)**:15–35.

[3] Holthusen, H., Brepols, T., Reese, S. and Simon, J.-W. A two-surface gradient-extended anisotropic damage model using a second order damage tensor coupled to additive plasticity in the logarithmic strain space. *Journal of the Mechanics and Physics of Solids* (2022) **163**:104833.

[4] Holzapfel, G. A., Gasser, T. C. and Ogden, R. W. A new constitutive framework for arterial wall mechanics and a comparative study of material models. *Journal of elasticity and the physical science of solids* (2000) **61**: 1–48.

[5] Manjunatha, K., Behr, M., Vogt, F. and Reese, S. A multiphysics modeling approach for in-stent restenosis: Theoretical aspects and finite element implementation. *arXiv*, doi: 10.48550/ARXIV.2204.02301 (2022).

[6] Manjunatha, K., Behr, M., Vogt, F. and Reese, S. Multi-physics modeling of in-stent restenosis. *Proceedings of the 7th International Conference on Computational and Mathematical Biomedical Engineering, 27–29 June 2022, Italy* (2022), 552–555.

[7] Parry, T., Thyagarajan, R., Argentieri, D., Falotico, R., Siekierka, J. and Tallarida, J. T. Effects of drug combinations on smooth muscle cell proliferation: An isobolographic analysis. *European Journal of Pharmacology* (2006) **532**:38–43.